Control Engineering Practice 123 (2022) 105140

Contents lists available at ScienceDirect

Control Engineering Practice

journal homepage: www.elsevier.com/locate/conengprac

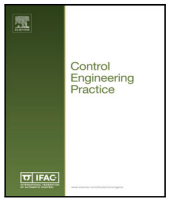

Model Predictive Control of the Mojave solar trough plants

Antonio J. Gallego [a,*], Manuel Macías [b], Fernando de Castilla [b], Adolfo J. Sánchez [a], Eduardo F. Camacho [a]

[a] Departamento de Ingeniería de Sistemas y Automática, Universidad de Sevilla, Camino de los Descubrimientos s/n., 41092 Sevilla, Spain
[b] Atlantica Sustainable Infrastructure, Albert Einstein s/n, 41092 Sevilla, Spain

ARTICLE INFO

Keywords:
Solar energy
Model Predictive Control
Solar trough
Large scale

ABSTRACT

The size of the current commercial solar trough plants poses new challenges in the applications of advanced control strategies. Ensuring safe operation while maintaining the temperature around an adequate set-point can lead to substantial gains in power production. Furthermore, the controller has to take into account the steam generator constraints to avoid trips leading to production losses.

Model Predictive Control algorithms have proved to perform well when controlling solar trough plants. In particular, many MPC strategies were developed and tested at the old experimental solar trough plant of ACUREX at the Plataforma Solar de Almería with excellent results.

In this paper, a Model Predictive Control algorithm is presented to control the average temperature of the large scale solar trough plants Mojave Alpha and Mojave Beta. This controller takes into account steam generator constraints in order to ensure safe operation. Several tests under different conditions have been carried out at the actual plants. Results show that the controller performs well on clear and cloudy days in spite of the great size of these plants.

1. Introduction

Most of the electricity produced comes from fossil fuels, nuclear and non-renewable energy sources (Heeckt & Kolaric, 2020). The use of clean and renewable energy sources becomes essential to reduce the negative environmental impact of fossil fuel energies. Solar energy is the most abundant renewable energy source (Blanco & Santigosa, 2017). Another important reason to use renewable energy sources is that fossil fuels will eventually become depleted (Shahzad, 2015). Many solar energy plants have been constructed around the world using different technologies: Photovoltaics, solar furnaces, solar tower, parabolic trough etc (Islam et al., 2018). This paper focuses on the parabolic trough technology.

Since 1980, solar energy plants are one of the fastest growing ways of harnessing renewable energy sources. Many solar projects have been built and commissioned around the world. For example, the 30 MW SEGS solar trough plants in the USA were commissioned in the 80s (SolarPaces, 2017). Later, multiple projects of solar trough plants can be found around the world (SolarPaces, 2019): the 50 MW solar trough plants of Helios I and II in Ciudad Real (Spain), Helioenergy I and II in Écija (Sevilla) all of them owned by Atlantica Sustainable Infrastructure (NREL Helios, 2020). Bigger solar trough plants have been constructed and connected to the grid since 2010. The SOLANA power plant commissioned in 2013 is a 280 MW solar trough plant with thermal storage (National Renewable Energy Laboratory (NREL), 2021b). In December 2014, the Mojave solar project was commissioned. It consists of two solar trough plants Mojave Alpha and Beta of 140 MW of net power production each (National Renewable Energy Laboratory (NREL), 2021a).

The use of solar energy has to face several challenges (N. A. Engineering, 2008). One of them is to make it economical and competitive as stated by the European Comission (2015). One of the ways of improving their competitivity is the application of advanced control strategies (Badal et al., 2019; Camacho & Gallego, 2013; Islam et al., 2018). The operation of solar trough plants is becoming more difficult as their size keeps increasing. The operators have to be aware of multiple signals coming from the field and the steam generator. Control algorithms that automatize some parts of the operation will help to improve the overall operation avoiding production losses.

A solar trough plant consists of a field of parabolic trough loops which collect the solar radiation and concentrate it onto a tube where synthetic oil passes through. The oil is then sent to a steam generator which produces steam to move turbines to produce electricity. If the plant has thermal storage units such as SOLANA or KAXU SOLAR ONE trough plants, the excess of thermal energy can be sent to be accumulated in the storage and used when needed (Yang et al., 2010).

* Corresponding author.
E-mail addresses: agallego2@us.es (A.J. Gallego), manuel.macias@atlantica.com (M. Macías), fernando.decastilla@atlantica.com (F. de Castilla), asanchezdelpozo@us.es (A.J. Sánchez), efcamacho@us.es (E.F. Camacho).

https://doi.org/10.1016/j.conengprac.2022.105140
Received 6 April 2021; Received in revised form 20 February 2022; Accepted 22 February 2022
Available online 11 March 2022

One of the main control objectives in solar trough plants is regulating the average temperature of the solar field around a desired temperature set-point by using the pump flow as a manipulated variable (Andrade et al., 2013; Camacho et al., 2019; Lima et al., 2016). As far as power production is concerned, the higher the temperature, the higher the efficiency of the Rankine cycle, but it is very important to consider the flow needed to reach the desired temperature. Higher temperatures imply higher thermal losses thus reducing the efficiency of the solar field as explained in Camacho and Gallego (2013). The computation of the optimal temperature is out of the scope of this work, and the working temperature is chosen by the operators and plant engineers based on their experience.

A solar trough plant is a highly nonlinear system with multiple disturbance sources affecting the field: the inlet temperature, the changes in environmental conditions and optical efficiencies and most important, the solar radiation disturbances (Camacho et al., 2012). Many of the control strategies designed for solar trough plants were developed for the old ACUREX solar field located at the Plataforma Solar de Almería (Camacho et al., 2007; Khoukhi et al., 2015; Rubio et al., 2006; Sánchez et al., 2018). This plant has been used extensively as a test-bench for testing control algorithms. However, current commercial solar trough plants cover great areas of land. For example, the two 140 MW solar trough plants of Mojave Alpha and Beta are composed of 282 loops each and cover about 700 hectares of land (Power Technology, 2015). The solar trough plant of SOLANA is even bigger: it covers about 780 hectares of land and it consists of 808 loops (National Renewable Energy Laboratory (NREL), 2021b).

The main contribution of this paper is the design and application of a Model Predictive Control strategy for controlling the average temperature of the large scale Mojave solar plants. Similar MPC strategies have been applied only to small scale solar plants such as the ACUREX field (Camacho & Gallego, 2015). The controller regulates the average temperature of the solar field around a set-point chosen by the operators by computing a set-point for the RPM of the main pumps. In this case, the average temperature is computed as the average outlet temperature of all the operative loops discarding those that are out of service. The controller is installed and used at present by the plant operators.

The main differences between controlling large scale solar trough plants and small scale solar plants can are:

- The steam generation imposes constraints to the RPM reference: the controller has to take into account constraints such as the steam pressure, the superheating value and the steam temperature gradient. The controller must take into account these constraints when computing a value for the RPM. This issue is not considered in general in experimental plants or simulation tests but it is of utmost importance in commercial plants: a violation of any of these constraints may produce a trip and involves a production loss (Gallego, Macias, et al., 2019).
- The great size of the current solar trough plants poses new challenges to the development and tuning up control strategies. One of them is that knowing the optical efficiency is very difficult since reflectometers offer only a local measure of the reflectivity (Sánchez et al., 2019).
- The use of the measurement of solar radiation provided by pyrheliometers is not a reliable one when transients are affecting one part of the field while the rest is not covered by clouds (Gallego & Camacho, 2012).
- Another important topic is that when the size increases the plant dynamics becomes slower with large time delays at low oil flow rates.

In order to address the issues stated above, the Advanced Grant Optimal Control of solar energy systems (OCONTSOLAR) funded by the European Research Council is currently continuously contributing to the solution of these challenges (European Comission, 2018).

Table 1
List of Abbreviations.

DNI	Direct normal irradiation
GS-GPC	Gain Scheduling Generalized Predictive Controller
HTF	Heat Transfer Fluid
MPC	Model Predictive Control
PDE	Partial Differential Equation
PID	Proportional+integral+derivative controller
RPM	Revolution per minute

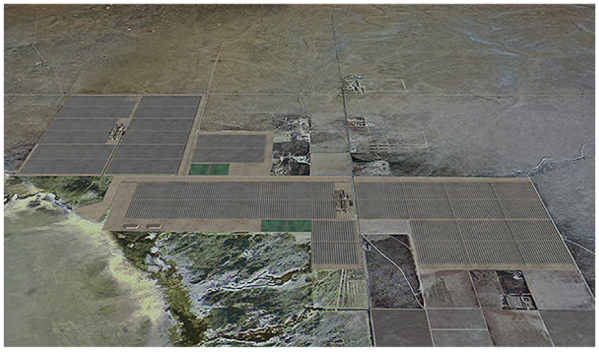

Fig. 1. Mojave solar project: Courtesy of Atlantica Sustainable Infrastructure.

The paper is organized as follows: Section 2 describes the Mojave solar plants. Section 3 presents a concise description of the mathematical model used to tune the controller, more details of the plant model are given in Gallego, Macias, et al. (2019). Section 4 develops the Model predictive control algorithm used and the constraints that it takes into account. Section 5 presents the results of the controller at the actual Mojave solar plants Alpha and Beta. Finally the paper finishes with concluding remarks (see Table 1). .

2. Description and mathematical model of the Mojave solar plants

In this section, a brief description of the Mojave Solar Project is presented. Next, the mathematical model of the plant is outlined since it has been fully described in Gallego, Macias, et al. (2019).

The Mojave solar project is a solar thermal project composed of two solar trough plants. It is located near Barstow in California (USA) and can produce up to 280 MW of net electrical power. Fig. 1 shows a panoramic view of the Mojave Solar Project (Power Technology, 2015).

The United States Environmental Protection Agency had the objective that 33% of the overall electricity produced in California should come from renewable energy sources (Agency, 2021). Mojave solar project aimed at fulfilling this objective by satisfying the electrical demand of 75000 homes approximately thus preventing the emission of 423800 tons of CO2 to the atmosphere (Agency, 2021).

As previously stated, the Mojave Solar Project consists of two parabolic trough solar plants, Mojave Alpha and Mojave Beta, each of 140 MW net power production. Both plants are formed by 282 parabolic trough loops covering about 780000 m^2. The reflective surface concentrates the direct solar radiation onto a metal tube where a synthetic oil circulates. The oil collects the energy, gets heated up and then used in a conventional steam generator and turbine to produce electricity (Fig. 2). It is worth pointing out that all the electrical energy produced is 100% provided by the sun. The plants do not use natural gas or other non renewable energy sources.

Mojave solar project was commissioned in December 2014 (Gallego, Macias, et al., 2019; Power Technology, 2021).

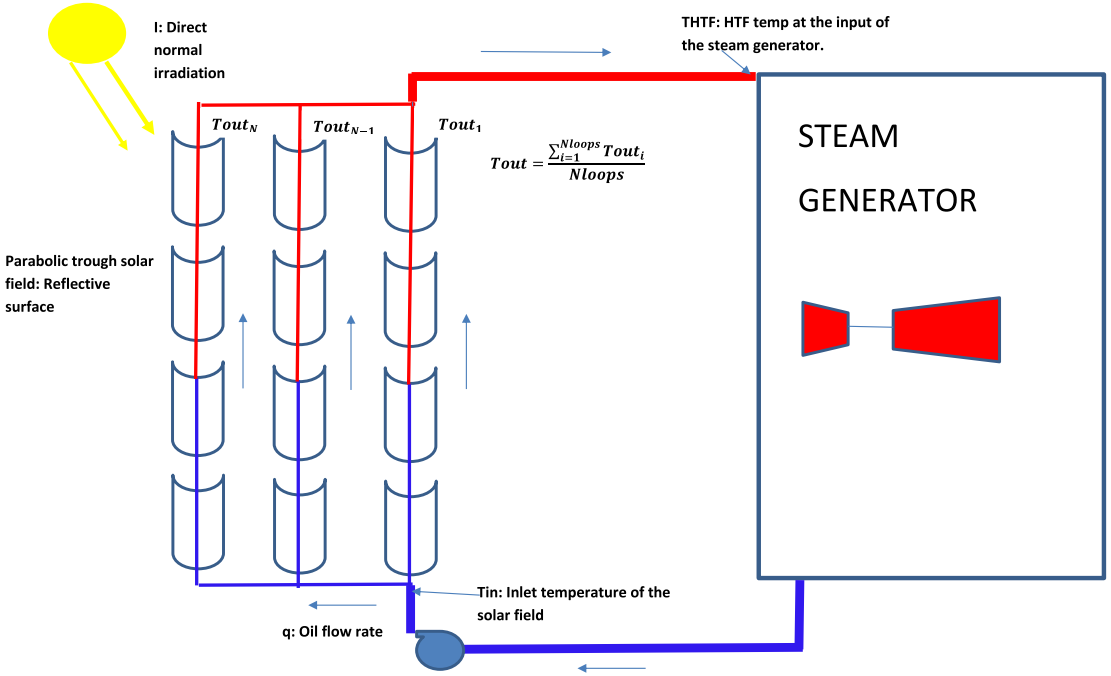

Fig. 2. Overall plant scheme.

2.1. Distributed parameter model of a loop

In this subsection, the mathematical model of a loop from Mojave solar plants is presented. The full model of the plant is completely described in Gallego, Macias, et al. (2019).

A loop from the Mojave Solar Plants consists of four collectors of 125 m each connected in series. The collectors are joined by tubes and joints (passive parts) where the solar irradiance does not reach. The whole plant can be modeled by adding loops in parallel. The distributed parameter model is used to simulate the plant and to obtain the parameters for the MPC control strategy.

The equations for the distributed parameter model have been widely used in literature (Alsharkawi, 2017; Camacho et al., 2012; Carmona, 1985; López-Bautista et al., 2020). The model is formed by two partial differential equations (PDE) which describe the energy balance in time and space.

$$\rho_m C_m A_m \frac{\partial T_m}{\partial t} = I K_{opt} cos(\theta) G - H_l G(T_m - Ta)$$

$$-LH_t(T_m - T_f)$$

$$\rho_f C_f A_f \frac{\partial T_f}{\partial t} + \rho_f C_f q \frac{\partial T_f}{\partial x} = LH_t(T_m - T_f) \quad (1)$$

The subindexes m and f stand for metal and fluid respectively. Table 2 describes the parameters and units of the distributed and concentrated parameter model.

The density and specific heat of the oil depend on the working temperature. They can be approximated by the following expressions. The parameters have been obtained using data from the manufacturer:

$$\rho_f = 1061.5 - 0.5787\ T - 9.0242e-4\ T^2$$
$$C_f = 1552.049 + 2.38501\ T + 0.0010558\ T^2 \quad (2)$$

The thermal losses coefficient was obtained by using real data from the field. It can be approximated by the following expression (Gallego, Macias, et al., 2019):

$$H_l = 11.7e-9\ (\Delta T)^3 - 2.81e-6\ (\Delta T)^2 + 1.44e-4\ \Delta T$$

Table 2
Parameter description.

Symbol	Description	Units
t	Time	s
l	Space	m
ρ	Density	kgm^{-3}
C	Specific heat capacity	$JK^{-1}kg^{-1}$
A	Cross sectional area	m^2
$T(l,t)$	Temperature	K,°C
$q(t)$	Oil flow rate	m^3s^{-1}
$I(t)$	Direct Solar Radiation	Wm^{-2}
$cos(\theta)$	Geometric efficiency	Unitless
K_{opt}	Optical efficiency	Unitless
G_a	Collector aperture	m
$T_a(t)$	Ambient temperature	K,°C
H_l	Coefficient of thermal loss	$Wm^{-2}°C^{-1}$
H_t	Coefficient of heat transmission metal–fluid	$Wm^{-2}°C^{-1}$
L	Perimeter of the pipe line	m
S	Total reflective surface	m^2
C_{th}	Thermal capacity of the solar field	J/K
Pc_p	Parameter of solar field	$J\ m^{-3}K^{-1}$
$\bar{T}$	Average between outlet and inlet temperatures	°C,K

$$+ 0.081 - \frac{3.21}{\Delta T}$$
$$\Delta T = T_m - T_a \quad (3)$$

Obtaining the expression of this coefficient involves using complex convection heat transmission formulas (Akbarzadeh & Valipour, 2018). Only the final expressions are given:

$$Hv(T) = 7.182817e-7 T_f^4 - 1.356114e-3 T_f^3 + 0.267921 T_f^2 + 479.1142 T_f + 5.011334e3$$

$$H_t = Hv(T) q^{0.8}\ (W/(m^2\ °C)) \quad (4)$$

To compute the geometric efficiency ($cos(\theta)$), the formulas explained in Duffie and Beckman (1991), Gallego et al. (2016) are used. It is difficult to know the optical efficiency K_{opt} since it is formed by parameters such as reflectivity, metal absorptance, transmittance etc

which are difficult to estimate. It was obtained by using data from the plant.

To solve the PDE system the forward Euler method is used with an integration step of 0.5 s. It was found that dividing the metal tube into 260 segments provides a good trade-off between accuracy of the model and computational time (Gallego, Macias, et al., 2019).

2.2. Concentrated parameter model

The concentrated parameter model provides a lumped description of the whole field. The variation in the internal energy of the fluid can be described by the equation (Camacho et al., 2012):

$$C_{th}\frac{dT_{out}}{dt} = K_{opt}cos(\theta)SI - qPc_p(T_{out} - T_{in}) - H_lS(\bar{T} - T_a) \quad (5)$$

Where T_{out} is the average of the outlet temperature of all the loops of the plant and T_{in} is the inlet temperature of the solar field. The rest of the symbols are explained in Table 2.

The concentrated parameter model has the advantage of its simplicity, but it has two main drawbacks. Firstly, it does not take into account the dependency of the temperature on the length of the tube because it considers the loop as a point. The variations in the inlet temperature are immediately reflected on the outlet temperature (Álvarez et al., 2010). In the actual loop, a variation in the inlet temperature affects the outlet temperature after circulating through the tube. The delay depends on the flow value. Secondly, it does not take into account the metal–fluid heat transfer process. However, this model produces good results for determining steady state conditions and is used to obtain a series feedforward compensator.

3. Model predictive control algorithm

This section presents the model predictive control algorithm designed for the Mojave solar plants. First, the mathematical formulation of the Model predictive control (Camacho & Bordons, 2004) is described. Then, some remarks are given about the constraints that the controller has to fulfill. The controller details cannot be fully disclosed due to confidentiality issues.

An MPC control strategy has been selected for two reasons: firstly, the prediction capabilities of the MPC have demonstrated to be very effective when controlling this kind of systems. Secondly, the control strategy has to fulfill constraints in the manipulated variable (the pumps RPM) and in the HP Pressure. A model for predicting the future values of the HP pressure is used based on the future values of the oil flow. The main advantage of the MPC is that the control strategy can be posed as a constrained optimization problem not only to fulfill the control objectives but also to satisfy the imposed constraints (Rawlings & Mayne, 2009).

Addressing these issues using other simpler control strategies such as a PID controller would be more complicated, since it does not provide a prediction of the future evolution of the control actions but computes the control for the current instant. To satisfy the constraints, a model of the control loop PID+system would be needed to predict the future evolution of the flow and temperature and, in turn, to predict the evolution of the HP Pressure in an constrained optimization problem.

The general formulation of an MPC control problem can be posed as follows:

$$\min_{\Delta u} J = \sum_{t=1}^{N_p}\left(y_{k+t|k} - y^{ref}_{k+t}\right)^{\intercal}\left(y_{k+t|k} - y^{ref}_{k+t}\right) + \lambda\sum_{t=0}^{N_c-1}\Delta u^{\intercal}{}_{k+t|k}\Delta u_{k+t|k}$$

s.t.

$$y_{k+t|k} = f(\Delta u, y_{k+t-1}, y_{k+t-2}, \ldots)$$
$$u_{k+t|k} = u_{k+t-1|k} + \Delta u_{k+t|k}$$
$$u_{\min} \le u_{k+t|k} \le u_{\max}$$
$$t = 0, \ldots, N_p - 1$$

N_p is the prediction horizon and N_c is the control horizon. The parameter λ penalizes the control effort. These are the parameters to be adjusted to obtain adequate performance at the actual plant.

Although a sequence of the control actions are computed to minimize the cost function, a receding horizon policy is used (Khoukhi et al., 2015). This means that only the first term of the calculated sequence is applied to the system and all the sequence is recalculated every sampling time.

In the next subsections, the models used to predict the evolution of the plant variables are described. As mentioned in the introduction, although the main function of the controller is regulating the average outlet temperature of the loops (called in this paper Tout) around a desired set-point, it can also take into account some constraints of the steam generator in order to avoid unsafe situations which may lead to trips and production losses. The controller is designed to be used after the start-up stage and up to the end of the operation.

It is important to note that the mathematical models used for the MPC strategy have to be as simple as possible: since the final version of the controller is to be installed in a centralized server, the computational burden has to be low. Two kinds of model are used: first the model to predict the future evolution of the field temperature and second the model to predict the evolution of the steam generator HP pressure.

3.1. Model to predict the average temperature of the solar field evolution

In this subsection, the model to predict the future evolution of the outlet temperature of the solar field is presented. One of the possibilities is to use a nonlinear model such as the one described by the system of Eqs. (1). It has been found that the resulting MPC optimization problem consumed far more time than using the solution proposed. This could have produced problems when the final version of the controller was installed in the server. This choice was ruled out.

Another option considered was using a simple linear model for control purposes. However, in order to obtain a good behavior in the entire operation range of the plant, a low gain controller should be used which is not desirable: a fast response without an inadequate oscillatory behavior is required.

To predict the evolution of the average temperature, the MPC controller uses a gain-scheduling approach similar to that explained in Gallego, Merello, et al. (2019): a linear CARIMA model is used to describe the joint response of a series feedforward compensator and the plant at different operating points.

The feedforward controller helps in two ways, by rejecting the measurable disturbances affecting the field and linearizing the behavior of the solar plant (Alsharkawi & Rossiter, 2017; Camacho et al., 1992; Li et al., 2020). By using this strategy, the mathematical model to predict the evolution of the set feedforward+plant can be assimilated to a linear transfer function (Camacho et al., 1994).

The feedforward is computed using the concentrated parameter model as follows:

$$q = \frac{(K_{opt}cos(\theta)SI - H_lS(\bar{T} - T_a))}{Pc_p(Tr - T_{in})} \quad (6)$$

Although a series feedforward is used, the plant dynamics greatly depend on the oil flow rate. In this paper, six linear models have been identified for six values of the oil flow covering the whole range of operation. In order to obtain the transfer function for a particular point, a linear interpolation is used. These models have been obtained by a linear regression applying a PRBS signal to the input of the feedforward in series with the mathematical model of the plant. It is considered that all the loops receives the same flow, radiation and the optical efficiency is perfectly known.

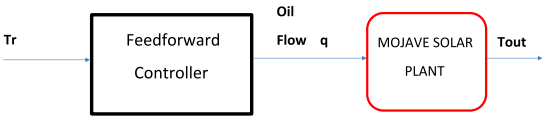

Fig. 3. Gain scheduling scheme: identification of linear models.

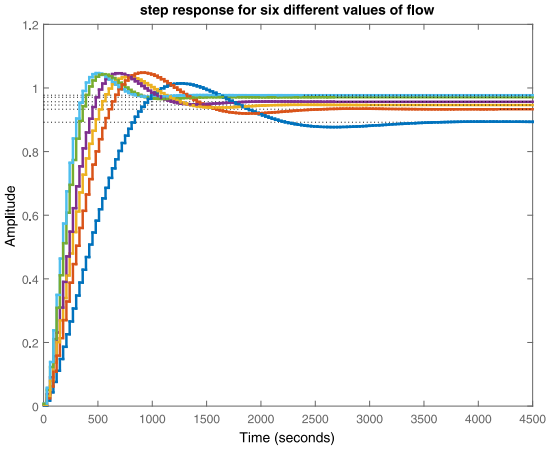

Fig. 4. Step response for different flow levels of Mojave Beta Plant.

In the gain scheduling scheme, the linear model computes the temperature reference Tr for the feedforward so that the average temperature of the solar field tracks the desired reference. Notice that this temperature does not have to be the same as the average temperature reference for the actual solar field. Notice that if the model were perfect, Tr would be the same as the average temperature reference in steady state. But, since the model is not perfect and there are mismatches between the real plant and the model, the MPC controller corrects these mismatches by modifying Tr (Camacho et al., 1994).

The following scheme shows how the gain scheduling scheme works (see Fig. 3).

The transfer function expression is as follows:

$$G(z^{-1}) = \frac{b_o + b_1 z^{-1} + b_2 z^{-2} + b_3 z^{-3} + b_4 z^{-4} + b_5 z^{-5} + b_6 z^{6}}{1 + a_o z^{-1} + a_1 z^{-2}} \tag{7}$$

Where the high order of the numerator aims at modeling high frequency dynamics of the plant that low order numerators cannot (Pickhardt, 2000). Despite what appears to be a conflict with simplicity, notice that the simplicity that is looked for is from the point of view of the computational time: the time invested in evaluating a linear difference equation of order six is negligible compared to the time invested in solving the constrained optimization problem.

The input to the transfer function is Tr and the output is the outlet temperature of the solar field (Gallego, Merello, et al., 2019).

Fig. 4 shows the step response for the obtained linear models from the slowest model (lowest flow value) to the fastest model (highest flow value).

The main uncertainty is in the time constants which vary from 180 to 500 s approximately. However, notice that the uncertainty is higher when dealing with the real plant. The optical efficiency of the whole plant is unknown producing that the gain uncertainty is higher. The flow balance is not perfect either: several loops may receive more flow than others producing different behaviors. Furthermore, not all loops receive the same level of solar radiation.

The sampling time is selected as 30 s. This sampling time is high enough to solve the MPC problem and is adequate for grasping the plant dynamics (time constants between 200 and 600 s) (Aström & Wittenmark, 1997; Lima et al., 2016).

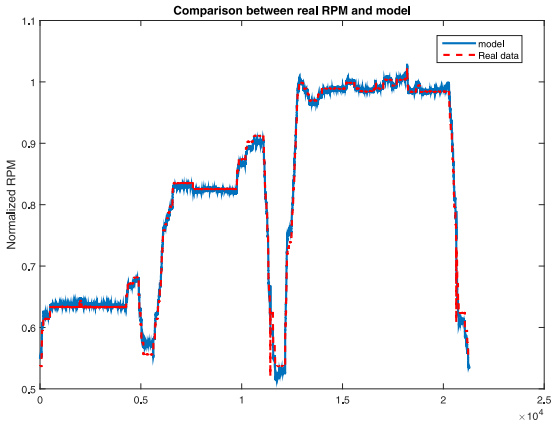

Fig. 5. RPM model: comparison with real plant data.

Once the flow rate has been obtained, the final step is to compute the RPM for the main pumps. The relation used to compute the RPM of the main pumps when the flow is known can be approximated as follows:

$$RPM = a_1 q + a_2 \tag{8}$$

This equation has been obtained by using data from the actual pumps. As can be seen in Fig. 5 the approximation error is negligible.

3.2. Steam generator constraints

In this subsection, the model used to predict the future evolution of the HP Pressure is presented.

If any of the variables of the steam generator are close to the maximum allowable value, the temperature regulation becomes a secondary objective. The most important issue is operation safety. The RPM set-point is computed to maintain a safe operation and the temperature is controlled by the defocus mechanism (Sánchez et al., 2019). The defocus mechanism consists of an automatic control algorithm which defocuses the collectors slightly so that less radiation is collected thus avoiding overheating problems. The closer the temperature is to the maximum value the greater the defocus angle.

When operating the plant, if the high steam pressure (HP pressure) is close to the maximum value (configurable), the controller must act on the RPM to avoid an overpressure situation. To carry out this task, the controller measures the HTF temperature at the input of the steam generator and it predicts the future evolution of the steam temperature and thus, the HP Pressure by using a mathematical model.

The controller supervises the high-pressure side because it is the most limiting. The low-side pressure is related to the high-side pressure. The HP pressure is more restrictive as the plant staff pointed out. A safety valve is closed by an external system, when the high-side pressure exceeds the limit. A high number of valve actions in a short period of time can result in a trip situation.

The steam temperature of the power block can be obtained by using the following equation:

$$T_{steam}(k) = a_1 * T_{steam}(k-1) + a_2 T_{HTF} + a_3 q\ T_{HTF} + a_4 (T_{HTF} - T_a) + a_5 (T_{HTF} - T_a)^2 + a_6 \tag{9}$$

Where T_{HTF} is the oil temperature at the input of the steam generator, q is the main pumps HTF flow and T_a is the ambient temperature. Taking into account this prediction, the future evolution of the HP pressure ($PresHP$) can be obtained by using the following model (Eq. (10)):

$$PresHP(k) = a_1 T_{steam} + a_2 T_{steam}^2 + a_3 q\ T_{HTF} + a_4 \tag{10}$$

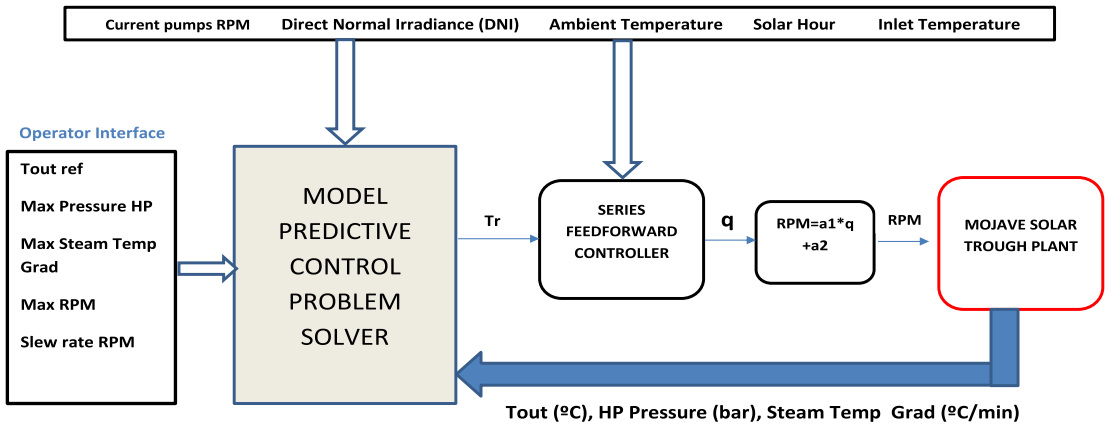

Fig. 6. Final Control Scheme.

The controller also supervises the steam temperature gradients. However, these variables are not controlled, only supervised. If these values are close to the maximum allowable values, the controller does not compute a new RPM set-point, it only updates the variables until the operator takes the appropriate actions to steer these variables within the safe range.

The main reason for acting in this way is that the control of these variables is performed far faster by manipulating valves in the steam generator without changing the RPM value. Furthermore, the steam temperature gradients are very important constraints that can produce trips if violated. The operator does not manipulate the RPM set-point but only the valves, and when the steam temperature gradients are within the safe range, the MPC resumes the computation of the RPM set-points starting from the current RPM value.

3.3. Constraints to be satisfied and final MPC scheme

Several values are configurable by the operators: the maximum and minimum value of the control signal (the RPM of the main pumps) as well as the slew-rate or maximum change of the RPM between every sampling time. The safe range for the steam temperature gradients and the maximum allowable HP Pressure are also configurable. When needed, the operators can change any of the constraints. The MPC solver takes these new values into account automatically.

Since the signal to be computed by the MPC control algorithm is the sequences of the Tr that solves the MPC problem, all the RPM constraints have to be posed as reference temperature constraints. To do this, the flow constraints with the RPM constraints can be obtained straightforwardly:

$$q_{max} = \frac{RPM_{max} - a_2}{a_1} \tag{11}$$

$$q_{min} = \frac{RPM_{min} - a_2}{a_1} \tag{12}$$

$$\Delta q = \frac{\Delta RPM - a_2}{a_1} \tag{13}$$

Once the flow constraints are obtained, the constraints for the Tr can be obtained by using the feedforward Eq. (6). The final MPC problem can be posed as follows:

$$\min_{\Delta Tr} J = \sum_{t=1}^{N_p} \left(Tout_{k+t|k} - T^{ref}_{k+t}\right)^{\intercal} \left(Tout_{k+t|k} - T^{ref}_{k+t}\right) + \lambda \sum_{t=0}^{N_c-1} \Delta Tr^{\intercal}_{k+t|k} \Delta Tr_{k+t|k}$$

s.t.

$$Tout_{k+t|k} = f(\Delta Tr, Tout_{k+t-1}, Tout_{k+t-2}, \ldots)$$

$$Tr_{k+t|k} = Tr_{k+t-1|k} + \Delta Tr_{k+t|k}$$

$$Tr_{\min} \leq Tr_{k+t|k} \leq Tr_{\max}$$

$$\Delta Tr_{\min} \leq \Delta Tr_{k+t|k} \leq \Delta Tr_{\max}$$

$$PresHP_{k+t|k} \leq PresHP_{\max}$$

$$t = 0, \ldots, N_p - 1$$

Where the function f is the discrete transfer function given by Eq. (7).

Given the sequence of the Tr computed by the MPC problem, the sequence of the oil flow can be obtained, thus obtaining a prediction of the future evolution for the $PresHP$. Notice that the maximum value for the $PresHP$ is posed as a hard constraint so that it has to be fulfilled.

The final control scheme works as follows (Fig. 6): at each sampling time, the Model Predictive Control problem solver block receives the plant variables: the inlet and outlet temperatures of the field, the HP pressure, the Steam Temperature Gradients, the direct normal irradiance, the current RPM value, ambient temperature and solar hour. It also receives from the operator interface the temperature reference for the solar field and the constraints to be satisfied.

The MPC solver block computes the Tr sequence to solve the optimization problem. Once the optimization problem is solved, the first element is used by the series feedforward to compute the flow rate and finally, the RPM set-point is obtained by means of Eq. (8).

4. Results

In this section, the results obtained with the proposed control strategy are shown. First, the procedure for adjusting the tuning parameters of the MPC is presented. Next, the results obtained at the actual plants with the controller are described and discussed. Data shown in this section has been scaled between 0–1 due to confidentiality issues. It is worth noting that the lower part of the figures, where the DNI and the pumps RPM are plotted, both of them scaled by the maximum value of the RPM for that day.

4.1. Simulation results

The MPC control algorithm was first tested on a nonlinear model of the Mojave solar plant (Gallego, Macias, et al., 2019). The values obtained for an adequate trade-off between performance and computational burden were: $N_p = 14$, $N_c = 7$ and $\lambda = 7$. These values were tuned by simulating several clear and cloudy days with data taken from the actual plant.

The first simulation was carried out using data from a clear day of February. The simulation consisted of a series of changing temperature references to test the tracking capabilities of the proposed control

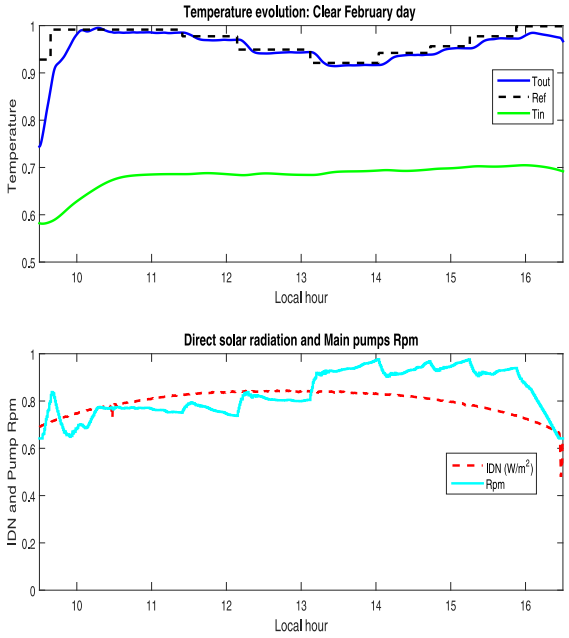

Fig. 7. Mojave Beta: first simulation. The test consists of several reference changes throughout a clear day.

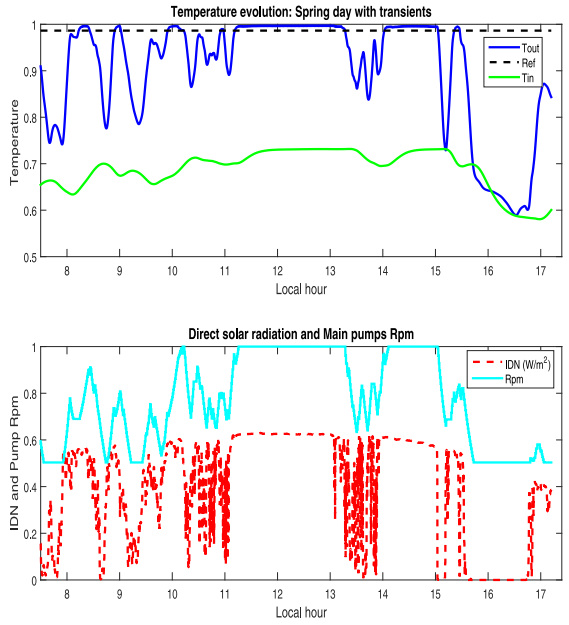

Fig. 8. Mojave Beta: second simulation. Spring day with strong radiation disturbances affecting the field.

strategy. As can be seen, the controller tracks well the temperature reference when possible (see Figs. 7 and 8).

The second simulation was carried out to test the behavior of the controller when strong radiation disturbances are affecting the field. As can be seen, the controller acts properly, increasing and decreasing the flow to steer the temperature close to the reference. There are two time intervals, from 11.2 to 13.1 h and from 14.1 to 15 h when the controller cannot reach the reference because the RPM set-point is at the maximum value.

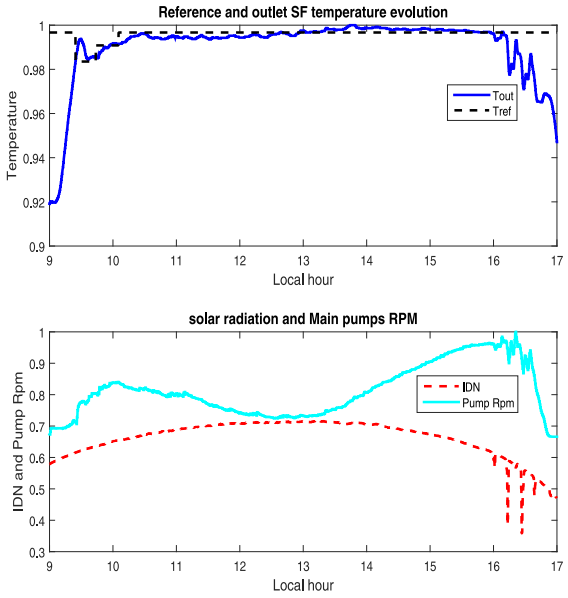

Fig. 9. Mojave Beta: clear day, constant temperature reference along the day.

4.2. Real plant results

In this subsection, results obtained with the proposed control strategy at the actual plants are presented. Several operation days of both Mojave Beta and Mojave Alpha are described below. After some preliminary tests, the final values for the controller parameters were $N_p = 16$, $N_c = 8$ and $\lambda = 8$ for both plants.

The controller was used by the operators choosing the values for the constraints and the temperature reference. It is worth pointing out that the controller operates the plant throughout the day without being switched off.

Figs. 9 and 10 show a clear day operation. The controller was connected after the start-up stage and the operator changes the set-point taking into account the operation and environmental conditions. They chose to slowly increase the reference to avoid an abrupt decrease in the flow. Then, the operators chose a constant reference temperature for the day.

As can be seen, the controller regulates around the desired set-point properly. It is worth pointing out that, since the controller is operating the solar field, the operator can invest more time in other plant issues.

Fig. 11 shows a clear day where the temperature reference changes. On this day, the operators change the set-point because the geometric efficiency changes throughout the day. Since the plant is oriented North–South, the cosine of the incidence angle reaches a minimum value at the solar noon (12 h solar time) (Gallego et al., 2016). Since the efficiency is lower at this hour, the operators change the set-point to avoid an excessive decrease in the oil flow, thus maintaining a good trade-off between flow and temperature. It is well known that maximum power production is not necessarily reached at higher temperatures (Camacho & Gallego, 2013).

As seen, the controller tracks the reference with a small overshoot. From 15.2 h to 16.5 h the controller cannot track the reference because the maximum RPM is reached. From 16.5 h onwards, the effective solar radiation is falling (end of the operation) and the solar field temperature cannot reach the set-point in spite of decreasing the RPM set-point.

Figs. 12 and 13 show a day when strong radiation disturbances are affecting both solar fields. The operators select a temperature reference for each plant and the controller manipulates the pumps RPM to track the set-point, if possible, and at the same time fulfill the slew-rate

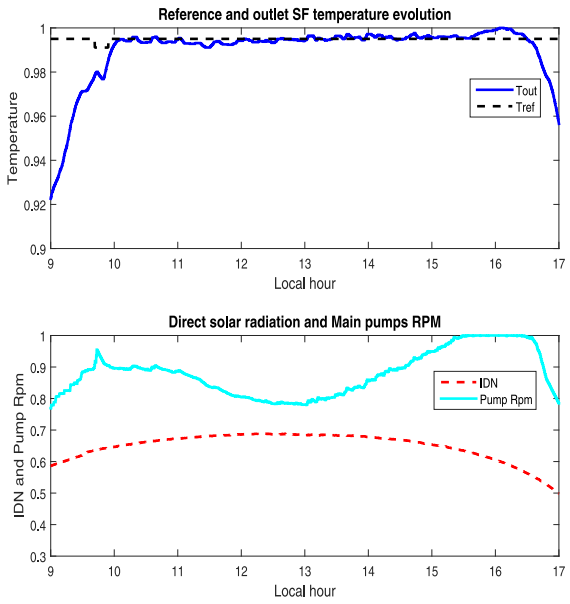

Fig. 10. Mojave Alpha: clear day, constant temperature reference along the day.

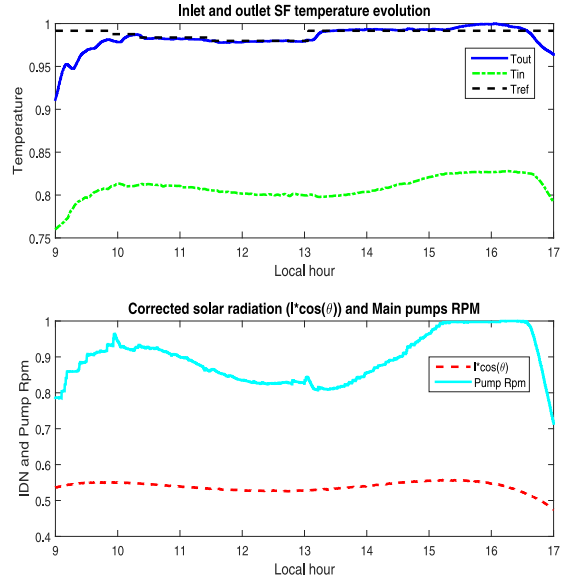

Fig. 11. Mojave Beta: clear day with changing temperature reference.

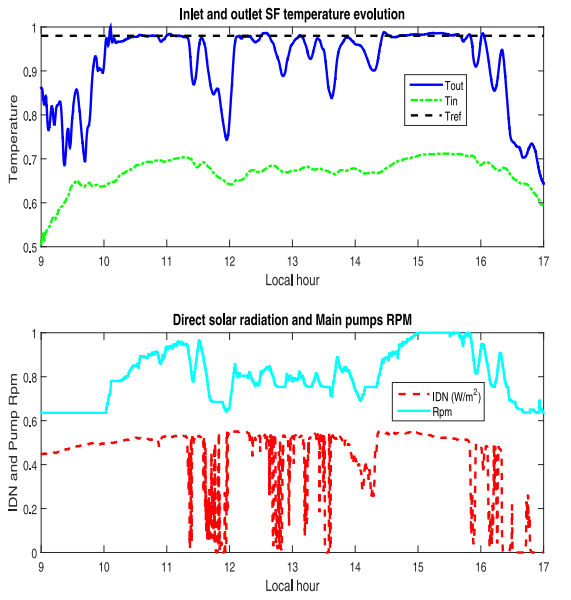

Fig. 12. Mojave Beta: Transients affecting the solar field.

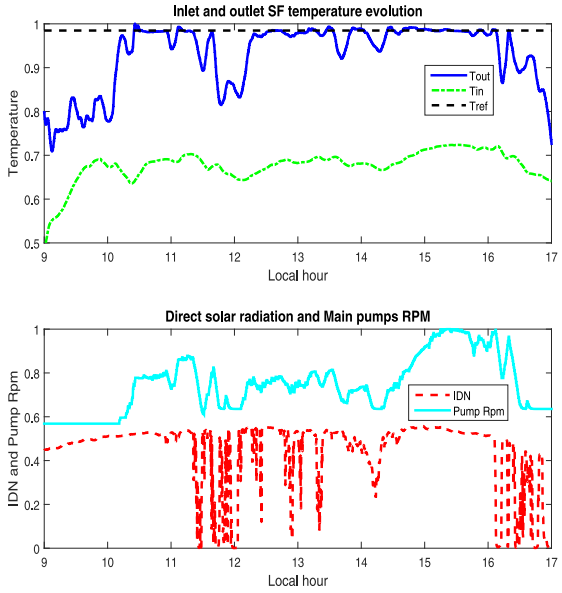

Fig. 13. Mojave Alpha: Transients affecting the solar field.

constraints. From 9 to 10 h the controller is at minimum flow because the outlet temperature is not close to the reference temperature.

From 11 to 14 h, strong radiation disturbances affect both fields. The controller acts on the RPM set-point trying to steer the outlet temperature close to the reference. As can be seen, the controller manages to track the set-point when possible. It is worth noting that, in spite of the measured solar radiation being quite similar in both fields, the evolution of the outlet temperature of both plants is different. This can be attributed to several factors. First, the difference in the overall efficiency of both plants, then, the solar radiation measurement is only a punctual one. Since the solar fields are quite large, the actual the solar radiation affecting the whole fields is not known. It is possible that the pyrheliometer is covered by a cloud and part of the field is not or vice versa. Moreover, which percentage of the field is affected by clouds is not known either.

Other remarkable behavior is that, in spite of the strong radiation changes, the controller does not produce an oscillatory behavior due to the excitation of the antiresonance modes. In both plants, the performance of the controller was considered very good by the operators.

Finally, the operation of a saturation day is shown in Fig. 14. On this kind of day, the controller cannot reach the set-point because there is more thermal energy in the solar field than the steam generator can absorb. The pumps RPM reached the maximum value but the solar field temperature is higher than the set-point.

On this kind of day, the temperature is controlled by the defocus algorithm in order to avoid overheating problems of the HTF, and the MPC controller supervises the steam generator constraints, in particular the high steam pressure.

Figs. 15 and 16 show the supervision of the HP Pressure. As can be seen in both figures, the controller acts on the RPM set-point to reduce the HP pressure when it is close to the maximum value configured by operators.

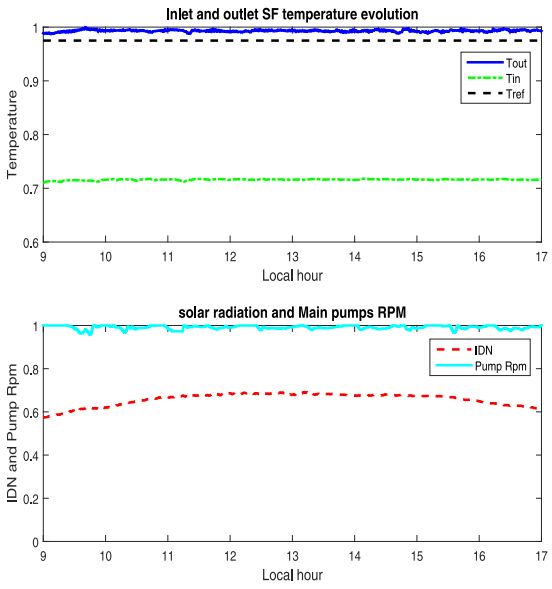

Fig. 14. Mojave Beta: Temperature regulation in a saturation day.

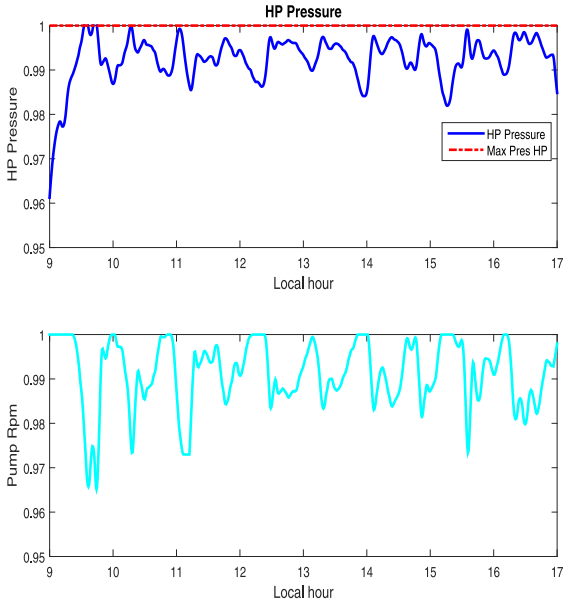

Fig. 15. Mojave Beta: Maximum HP pressure supervision in a saturation day.

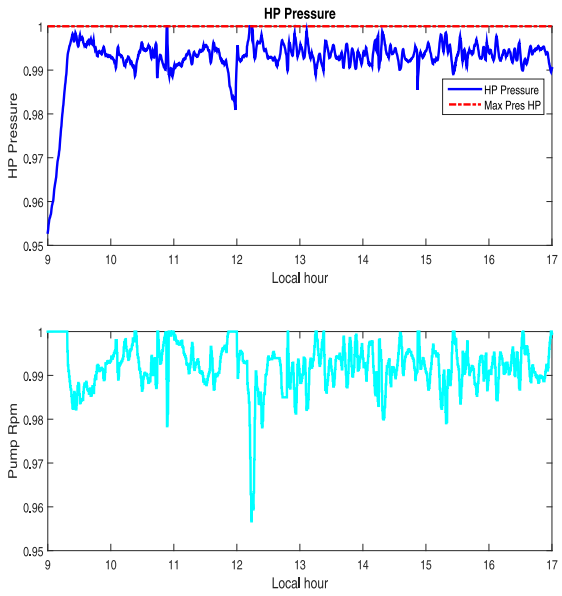

Fig. 16. Mojave Alpha: Maximum HP pressure supervision in a saturation day.

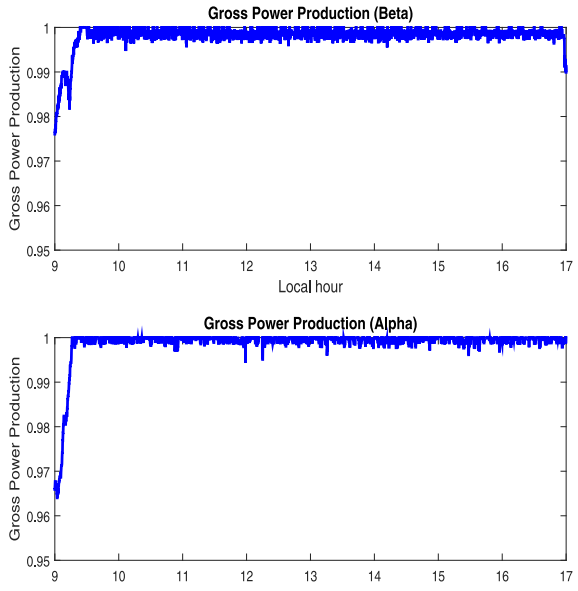

Fig. 17. Mojave Beta and Mojave Alpha.

Ensuring that the HP pressure does not surpass the maximum value is not an easy matter. Since the pumps are working at 100% of the speed variator, they sometimes have a problem in the hydraulic pressure that produces a sudden fall in the RPM, as seen at 12.1 h in Fig. 16. The controller avoids overpressure situations and ensures safe operation. Furthermore, the HP pressure is always above the 98.3% of the maximum allowable HP pressure without surpassing the maximum value.

Fig. 17 shows the gross power production in Mojave Beta and Alpha. As can be seen, both plants are almost at full production throughout the day.

5. Concluding remarks

Model Predictive Control algorithms have demonstrated to perform well when controlling solar trough plants. In particular, many MPC strategies have been developed and tested at the old experimental solar trough plant of ACUREX at the Plataforma Solar de Almería with excellent results.

In this paper, a Model Predictive Control algorithm is presented to control the average temperature of the large scale solar trough plants Mojave Alpha and Mojave Beta. This controller takes into account the main steam generator constrains in order to ensure safe operation.

Several real tests under different conditions have been carried out at the actual plants. Results show that the controller performance is satisfactory on clear and cloudy days. The controller performs well on clear days tracking the set-point given by the operator. On transient days, it manipulates the flow increasing and decreasing the pumps RPM, in order to maintain the outlet temperature close to the desired set-point. At the same time, it fulfills the constraints imposed by the operators.

The controller is currently installed and used by the plant operators with satisfactory opinions.

Declaration of competing interest

The authors declare that they have no known competing financial interests or personal relationships that could have appeared to influence the work reported in this paper.

Acknowledgments

The authors would like to thank Atlantica Sustainable Infrastructure for funding and collaborating in this work. The authors would like to acknowledge the European Research Council and the European Union for funding the work under the Advanced Grant OCONTSOLAR (Project ID: 789051).

References

Agency, U. S. E. P. (2021). Avoided emissions and generation tool (AVERT). URL https://www.epa.gov/avert.

Akbarzadeh, S., & Valipour, M. S. (2018). Heat transfer enhancement in parabolic trough collectors: A comprehensive review. *Renewable and Sustainable Energy Reviews*, *92*, 198–218.

Alsharkawi, A. (2017). *Automatic control of a parabolic trough solar thermal power plant* (Ph.D. thesis), University of Sheffield.

Alsharkawi, A., & Rossiter, J. A. (2017). Towards an improved gain scheduling predictive control strategy for a solar thermal power plant. *IET Control Theory & Applications*, *11*(12), 1938–1947. http://dx.doi.org/10.1049/iet-cta.2016.1319.

Álvarez, J. D., Costa-Castelló, R., Berenguel, M., & Yebra, L. J. (2010). A repetitive control scheme for distributed solar collector field. *International Journal of Control*, *83*(5), 970–982.

Andrade, G. A., Pagano, D. J., Álvarez, J. D., & Berenguel, M. (2013). A practical NMPC with robustness of stability applied to distributed solar power plants. *Solar Energy*, *92*, 106–122. http://dx.doi.org/10.1016/j.solener.2013.02.013.

Aström, K. J., & Wittenmark, B. (1997). *Prentice-Hall information and system sciences series*, *Computer-controlled systems: Theory and design* (3rd ed.). Upper Saddle River, NJ: Prentice-Hall.

Badal, F. R., Das, P., Sarker, S. K., & Das, S. K. (2019). A survey on control issues in renewable energy integration and microgrid. *Protection and Control of Modern Power Systems*, *4*(1), 8. http://dx.doi.org/10.1186/s41601-019-0122-8.

Blanco, M. J., & Santigosa, L. R. (2017). *Advances in concentrating solar thermal research and technology* (1st ed.). Woodhead Publishing, http://dx.doi.org/10.1016/C2014-0-04054-3.

Camacho, E. F., Berenguel, M., & Rubio, F. R. (1994). Application of a gain scheduling generalized predictive controller to a solar power plant. *Control Engineering Practice*, *2*, 227–238. http://dx.doi.org/10.1016/0967-0661(94)90202-X.

Camacho, E. F., Berenguel, M., Rubio, F., & Martínez, D. (2012). *Control of solar energy systems* (1st ed.). Springer-Verlag.

Camacho, E. F., & Bordons, C. (2004). *Model predictive control* (2nd ed.). Springer Verlag.

Camacho, E. F., & Gallego, A. J. (2013). Optimal operation in solar trough plants: a case study. *Solar Energy*, *95*, 106–117. http://dx.doi.org/10.1016/j.solener.2013.05.029.

Camacho, E. F., & Gallego, A. J. (2015). Model predictive control in solar trough plants: A review. In *5th IFAC conference on nonlinear MPC* (pp. 278–285). Sevilla (Spain): http://dx.doi.org/10.1016/j.ifacol.2015.11.296.

Camacho, E. F., Rubio, F. R., Berenguel, M., & Valenzuela, L. (2007). A survey on control schemes for distributed solar collector fields. Part II: advanced control approaches. *Solar Energy*, *81*, 1252–1272.

Camacho, E. F., Rubio, F. R., & Hughes, F. (1992). Self-tuning control of a solar power plant with a distributed collector field. *IEEE Control Systems*, *0272- 1708/92/*, 72–78.

Camacho, E. F., Sánchez, A. J., & Gallego, A. J. (2019). *Solar energy systems: Progress and future directions* (pp. 1–59). Nova Publishers, chapter Model Predictive Control of Large Scale Solar Trough Plants.

Carmona, R. (1985). *Análisis, Modelado y control de un campo de colectores solares distribuidos con sistema de seguimiento en un eje.* (Ph.D. thesis), Universidad de Sevilla.

Duffie, J., & Beckman, J. (1991). *Solar engineering of thermal processes* (2nd ed.). Wiley-Interscience.

European Comission (2015). Communication of the commission to the European parlament and the council concerning the Paris protocol-a blueprint for tackling global climate change beyond 2020. https://ec.europa.eu/commission/publications/paris-protocol-blueprint-tackling-global-climate-change-beyond-2020_en. (Accessed 1 May 2019).

European Comission (2018). Community research and development information service OCONTSOLAR. https://cordis.europa.eu/project/rcn/216250_es.html. (Accessed 1 May 2019).

Gallego, A. J., & Camacho, E. F. (2012). Estimation of effective solar radiation in a parabolic trough field. *Solar Energy*, *86*, 3512–3518.

Gallego, A. J., Macias, M., de Castilla, F., & Camacho, E. F. (2019). Mathematical modeling of the mojave solar plants. *Energies*, *12*(21), 4197. http://dx.doi.org/10.3390/en12214197.

Gallego, A. J., Merello, G. M., Berenguel, M., & Camacho, E. F. (2019). Gain-scheduling model predictive control of a fresnel collector field. *Control Engineering Practice*, *82*, 1–13. http://dx.doi.org/10.1016/j.conengprac.2018.09.022.

Gallego, A. J., Yebra, L. J., Camacho, E. F., & Sánchez, A. J. (2016). Mathematical modeling of the parabolic trough collector field of the TCP-100 research plant. In *9th EUROSIM congress on modelling and simulation*.

Heeckt, C., & Kolaric, S. (2020). *Urban sustainability in Europe: What is driving cities' environmental changes?*: *Technical report*, European Environment Agency, URL https://www.eea.europa.eu/publications/urban-sustainability-in-europe-what.

Islam, M. T., Huda, N., Abdullah, A. B., & Saidur, R. (2018). A comprehensive review of state of the art concentrating solar power (CSP) technologies: Current status and research trends. *Renewable and Sustainable Energy Reviews*, *91*, 987–1018. http://dx.doi.org/10.1016/j.rser.2018.04.097.

Khoukhi, B., Tadjine, M., & Boucherit, M. S. (2015). Nonlinear continuous-time generalized predictive control of solar power plant. *International Journal for Simulation and Multidisciplinary Design Optimization*, *A3*(6), 1–12. http://dx.doi.org/10.1051/smdo/2015003.

Li, L., Li, Y., & He, Y.-L. (2020). Flexible and efficient feedforward control of concentrating solar collectors. *Applied Thermal Energy*, *171*, http://dx.doi.org/10.1016/j.applthermaleng.2020.115053.

Lima, D. M., Normey, J. L., & Santos, T. L. M. (2016). Temperature control in a solar collector field using filtered dynamic matrix control. *ISA Transactions*, *62*, 39–49. http://dx.doi.org/10.1016/j.isatra.2015.09.016.

López-Bautista, A. O., Flores, A., & Gutiérrez-Limón, M. A. (2020). Robust model predictive control for a nanofluid based solar thermal power plant. *Journal of Process Control*, *94*, 97–109.

N. A. Engineering (2008). National academy of engineering. Grand challenges for engineering. URL www.engineeringchallenges.org. (Accessed 1 May 2019).

National Renewable Energy Laboratory (NREL) (2021a). Concentrating solar power projects. Mojave solar project. URL https://solarpaces.nrel.gov/project/mojave-solar-project. (Accessed 1 May 2019).

National Renewable Energy Laboratory (NREL) (2021b). Concentrating solar power projects. Solana generating station. URL https://solarpaces.nrel.gov/project/solana-generating-station. (Accessed 1 May 2019).

NREL Helios (2020). Concentrated solar power projects. Helios I. URL https://solarpaces.nrel.gov/helios-i.

Pickhardt, R. (2000). Adaptive control of a solar power plant using a multi-model control. *IEEE Proceedings Theory and Applications*, *147*(5), 493–500.

Power Technology (2015). Mojave solar thermal power facility, San Bernardino county, California. URL https://www.power-technology.com/projects/mojave-solar-thermal-power-california-us/.

Power Technology (2021). Mojave solar thermal power facility, san bernardino county, california. URL https://www.power-technology.com/projects/mojave-solar-thermal-power-california-us/.

Rawlings, J., & Mayne, D. (2009). In C. M. Rawlings (Ed.), *Model predictive control: Theory and design*. Nob Hill Publishing, LLC.

Rubio, F. R., Camacho, E., & Berenguel, M. (2006). Control de campos de colectores solares. *Revista iberoamericana de automática e informática industrial*, *3*(4), 26–45, URL https://polipapers.upv.es/index.php/RIAI/article/view/8158.

Sánchez, A. J., Gallego, A. J., Escaño, J. M., & Camacho, E. F. (2018). Temperature homogenization of a solar trough field for performance improvement. *Solar Energy*, *165C*, 1–9.

Sánchez, A. J., Gallego, A. J., Escaño, J., & Camacho, E. (2019). Adaptive incremental state space MPC for collector defocusing of a parabolic trough plant. *Solar Energy*, *184*, 105–114. http://dx.doi.org/10.1016/j.solener.2019.03.094.

Shahzad, U. (2015). The need for renewable energy sources. *ITEE Journal*, 16–18, URL https://www.researchgate.net/publication/316691176_The_Need_For_Renewable_Energy_Sources.

SolarPaces (2017). Csp project development. URL https://www.solarpaces.org/csp-technologies.

SolarPaces (2019). Concentrating solar power projects by country. URL https://solarpaces.nrel.gov/by-country.

Yang, Z., Suresh, & Garimella, V. (2010). Thermal analysis of solar thermal energy storage in a molten-salt thermocline. *Solar Energy*, *84*, 974–985. http://dx.doi.org/10.1016/j.solener.2010.03.007.